Bainite Transformation Temperatures in High-Silicon Steels

L.C. CHANG

The bainite transformation temperatures of eight high-silicon steels were determined metallographically. The bainite start (B_s) temperatures, which define the highest temperature at which bainite can form, all lay below the T_0 loci, where ferrite and austenite of the same chemical compositions have identical free energy. The established method of calculating B_s temperatures gave reasonable agreement with the experimental results. Careful study of the isothermally reacted samples revealed that Widmanstätten ferrite and bainite could both be observed, even at the beginning of the transformation, at around the B_s temperature. On the other hand, the lower bainite start (LB_s) temperatures of these steels were found to be very close to the martensite start (M_s) temperatures. Silicon is considered to be responsible for depressing the LB_s temperature by retarding the formation of cementite. The coformation of upper and lower bainite near the LB_s temperature is also confirmed. The results indicate that the displacive formation mechanism of bainite is sustainable.

I. INTRODUCTION

DESPITE having been studied extensively, bainite transformation in steels still remains the least understood of all the decomposition reactions of the high-temperature austenitic phase. Two opposite mechanisms have been proposed: diffusional and displacive reaction mechanisms.[1–4] By the diffusional reaction mechanism, the growth of bainitic ferrite is considered to take place by the diffusion-controlled movement of the ledge.[1,2,4] The carbon concentration of growing bainitic ferrite is in equilibrium with respect to austenite. The bainite reaction is, in fact, assumed to be an extension of the proeutectoid ferrite reaction. The bay in transformation-time-temperature (TTT) diagrams at the bainite start temperature and the well-known *incomplete transformation phenomenon* of bainite are explained in term of a *solute draglike effect* (SDLE), produced by the segregation of certain alloying elements into the mobile austenite/ferrite boundaries.[1,4] Those alloying elements (such as Mo) trapped in boundaries depress the carbon activity in austenite in contact with the growing ferrite, thereby reducing the diffusional flux of carbon into austenite and the resulting ferrite growth. This leads to growth stasis or the complete cessation of growth of bainite. The growth kinetics of some Fe-C-Mo alloys was reported to be influenced by the segregation of Mo in the austenite/ferrite boundary area, consistent with the SDLE hypothesis.[5,6] However, contradictory results of some other alloy systems were also reported.[3,7] On the other hand, the bainite transformation is postulated to occur diffusionlessly, as far as the solvent and substitutional atoms are concerned, by the displacive reaction mechanism.[1,3] Bainitic ferrite supersaturated with carbon forms displacively, with carbon diffusing from ferrite into austenite after the growth event or, alternatively, precipitating as a carbide inside the ferrite. As a displacive product, the highest temperature at which bainite can grow (B_s) should lie below the corresponding temperature of the T_0 curve, for which ferrite and austenite with identical chemical compositions have the same free energy.[8,9] The lower bainite start (LB_s) is the temperature below which lower bainite forms instead of upper bainite. It is suggested that the transition from upper to lower bainite is the kinetics competition between the carbon partition from ferrite into austenite and the carbide precipitation in ferrite.[10] Lower bainite will be absent when carbon depletion occurs before carbide precipitation in ferrite, and *vice versa*.

If, indeed, bainite grows displacively, only a limited amount of bainitic ferrite can form near the B_s temperature, according to thermodynamic considerations. The determination of the B_s temperature is straightforward if no other transformations such as pearlite and Widmanstätten ferrite, which can possibly grow around the B_s temperature, interfere. Otherwise, the determination of B_s temperature is difficult, although not impossible.[11] The morphology of Widmanstätten ferrite has a similar appearance to bainite, but the plates are thicker in size. Oblak and Hehemann[12] considered that the growth of Widmanstätten ferrite is proceeded by the continued advance of an interface. Bainite, on the other hand, grows by repeated nucleation of bainitic subunits. The two phases, nevertheless, have been suggested to have identical nucleation processes, but the growth event is different; bainite grows in a displacive manner, with excess carbon partitioning into the surrounding austenite soon afterward, while the growth of Widmanstätten ferrite, also diffusionless as far as the substitutional atoms are concerned, is controlled by the diffusion of carbon in austenite ahead of the advancing austenite/ferrite interface.[13,14]

Silicon is known to have the effect of retarding cementite precipitation, due to its extremely low solubility in cementite.[15] If the described theory of upper/lower bainite transition is correct,[10] it is expected that the presence of silicon will depress the formation temperature of lower bainite, since silicon prolongs the time needed for carbide precipitation.

The goal of this article is to report the B_s and LB_s temperatures of eight high-silicon steels. Emphasis will also be made on the coformation of bainite and Widmanstätten ferrite at the temperature near B_s and on the effect of silicon in depressing the formation temperature of lower bainite

L.C. CHANG, Associate Professor, is with the Department of Mechanical Engineering, Kuang-Wu Institute of Technology and Commerce, Taipei, Taiwan, 116, Republic of China.

Manuscript submitted February 19, 1998.

Table I. Chemical Compositions (Weight Percent) of the Experimental Alloys*

Alloy	C	Si	Mn	Ni	Cr
L1	0.095	1.63	1.99	—	1.97
L2	0.1	1.77	2.12	2.0	—
M1	0.27	1.98	2.18	—	1.9
M2	0.27	2.01	2.16	2.07	—
M3	0.26	1.85	2.10	—	—
M4	0.26	1.93	2.04	—	1.02
H1	0.46	2.10	2.15	—	—
H2	0.44	2.13	2.14	—	0.5

*The designations ''L,'' ''M,'' and ''H'' refer to low, medium, and high carbon steels, respectively.

(LB_s). It is hoped that this study can provide some evidence to elucidate the controversial mechanism of bainite transformation in steels.

II. EXPERIMENTAL

A. *Experimental Materials*

The chemical compositions of the experimental alloys are given in Table I. The alloys were made as vacuum melts in the Swinden Laboratories of British Steel (Sheffield, England). The as-cast ingots were forged and rolled into plates 16-mm thick by 150-mm wide. The alloys all contain sufficient silicon (about 2 wt pct) to prevent the precipitation of cementite during the transformation to bainite and about 2 wt pct of manganese for the purpose of hardenability. The carbon, nickel, and chromium concentrations are significantly different in order to obtain corresponding variations in the stability of the austenite. The steels were first machined into 10-mm-diameter rods, sealed in quartz tubes containing a partial argon atmosphere, and then given a homogenization heat treatment at 1300 °C for 3 days, followed by furnace cooling to room temperature. Samples were then machined from the homogenized specimens into cylindrical shapes, each 8 mm in diameter and 12 mm in length. To ensure rapid cooling, each cylinder was drilled to create a 3-mm-diameter longitudinal hole. The specimens were then nickel plated using a two-stage procedure, striking and plating. The striking process used a solution consisting of 250 g nickel sulfate and 27 mL concentrated sulfuric acid in 1 L of distilled water at 50 °C for 3 minutes, with a current density of 7.7 mA mm^{-2}. The plating was carried out at 50 °C for 15 minutes with a current density of 0.4 mA mm^{-2} in an electrolyte containing 140 g nickel sulfate, 15 g ammonium chloride, and 20 g boric acid in 1 L of distilled water.

B. *Dilatometry*

Isothermal transformation was performed in a Thermecmastor-Z (Fuji Electronic Industrial Company Ltd., Tsurugashimachi, Japan) thermomechanical simulator capable of monitoring the strain, load, time, and temperature during the course of transformation. The machine is equipped with an environmental chamber which can be evacuated using a rotary and oil-diffusion pump, or which can be filled with inert gas. The heat source is an RF coil, and the temperature was measured with a Pt/Pt-10 pct Rh thermocouple spot-welded to the sample. The temperature variation along the length of the sample was confirmed to be within 4 °C to 5 °C.

The samples were made austenitic by heating them to 1000 °C for 10 minutes in the vacuum chamber, then quenching them, using a nitrogen or helium jet, to a variety of isothermal temperatures below the bainite start temperature but above the martensite start temperature. The diameter change during transformation was recorded in order to relate this to the volume change on transformation, using a method described elsewhere in detail.[16] The B_s temperature is determined at the point where the volume fraction of bainitic ferrite formed is around 0.05.

C. *Optical Microscopy and Transmission Electron Microscopy*

The specimens were prepared for optical microscopy by mounting in conductive BAKELITE,* grinding using 120-grit silicon carbide paper, and, finally, polishing down to 1 mm using a diamond grit. They were etched using 2 pct nital. Thin foils for transmission electron microscopy (TEM) were prepared from 0.3-mm-thick discs machined from 8-mm-diameter rods. The discs were ground to 60- to 80-mm thickness by abrasion using SiC coated grinding paper and were electropolished in a twin-jet polishing unit containing an electrolyte of 5 pct perchloric acid, 25 pct glycerol, and 70 pct ethyl alcohol. The polishing potential was 55 V at a current of 20 to 30 mA, the electrolyte temperature being maintained in the range from −5 °C to −10 °C. The thin foils were examined using a PHILIPS** EM-400ST transmission electron microscope operated at 120 kV.

*BAKELITE is a trademark of Union Carbide Corporation, Danbury, CT.

**PHILIPS is a trademark of Philips Electronic Instruments Corp., Mahwah, NY.

III. RESULTS AND DISCUSSION

A. *Transformation Temperatures*

Extensive and routine metallography and dilatometric experiments were carried out to determine the upper and lower bainite transformation temperatures and the martensite start temperature (B_s, LB_s, and M_s, respectively). The studies were conducted at isothermal intervals of, at most, 20 °C, which, therefore, ensures their accuracy. The results are plotted against only the corresponding carbon concentration in Figure 1 and are tabulated at Table II.

B. *Bainite Start Temperatures*

It is known that transformation near the B_s temperature may involve not only bainite but also pearlite,[11] although the latter phase is more sluggish. In the presence of pearlite, the determination of B_s temperature is difficult, but not impossible. Five alloys in the present study have well-defined B_s temperatures, in which only a limited amount of bainite can form after a considerable period of time without the

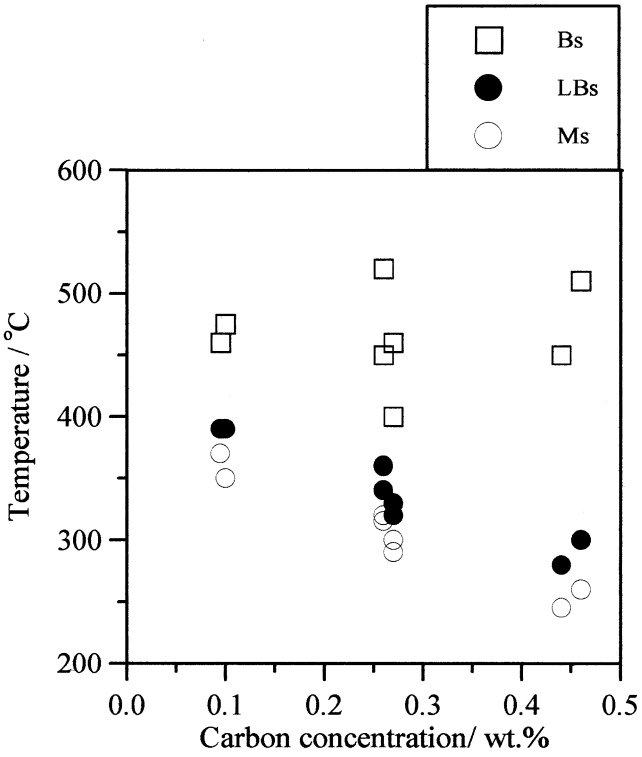

Fig. 1—The measured upper and lower bainite start temperatures and martensite start temperatures (listed in Table II), plotted as a function of the steel carbon concentration. Note that the substitutional solute of the steels within any carbon category are not identical (Table I).

Table II. The Measured Transformation Start Temperatures (°C)

Alloy	B_s	LB_s	M_s
L1	460	390	370
L2	480	390	350
M1	400	325	300
M2	460	330	290
M3	540	360	315
M4	450	340	320
H1	510	300	260
H2	450	280	245

interference of other phases. In this case, a clear bay can be observed in the TTT diagram.[17] Figure 2 shows a typical optical micrograph and TEM micrograph of alloy M2. It is noted that, after 2500 seconds of transformation, only a limited amount of bainitic ferrite can be observed optically. The discrete distribution of bainitic subunits (Figure 2(b)), contrary to the classic sheaf morphology which consists of numerous subunits when undercooling is greater, indicates that the nucleation event is the controlling factor in the formation of bainite near the B_s temperature. The absence of austenite films between bainitic subunits in Figure 2(b) may result from the high diffusivity of carbon as well as the discrete nature of ferrite morphology, both of which encourage the homogenization of carbon after completion of the bainitic ferrite formation.

At the determined B_s temperature (510 °C) of alloy H1, bainitic ferrite formed first, followed by the formation of pearlite along the grain boundary. Figure 3 shows the optical micrographs after 120 and 7200 seconds of reaction,

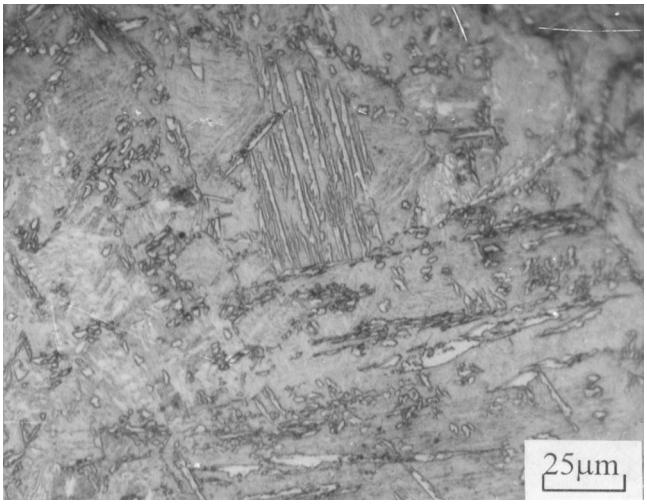

(*a*)

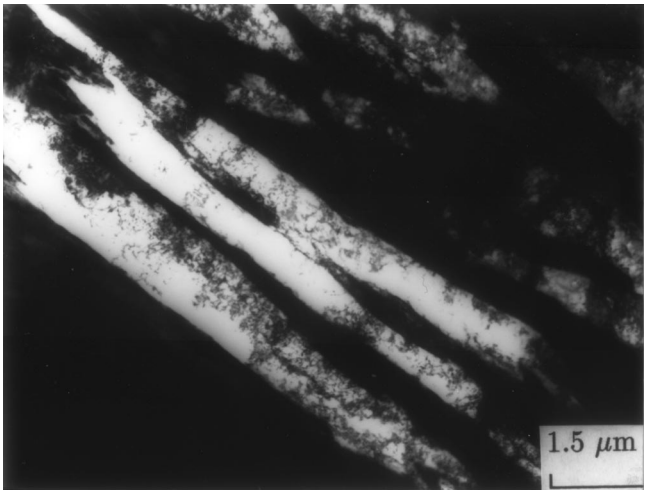

(*b*)

Fig. 2—Micrographs showing the microstructure of alloy M2 reacted at 460 °C for 2500 s: (*a*) optical image and (*b*) TEM bright-field image.

confirming that the formation of diffusional pearlite lags behind the displacive growth of bainitic ferrite. After long-term holding (7200 seconds), carbide also precipitated from the enriched austenite between bainitic ferrite (Figure 4). Two types of ferrite morphologies were observed at 510 °C before the interference of pearlite formation, as shown in Figure 5. The long lenticular laths of ferrite found in Figure 5(a) should be classified as upper bainite, bainitic subunits growing from the austenite grain boundary. The so-called *sympathetic nucleation* in the growth of bainite can be revealed: a submicron subunit B clearly nucleated and grew from the tip area of the already formed subunit A, which has been considered to be a favorable nucleation site.[18,19] The other distinctive ferrite morphology (Figure 5(b)), judging from its wedge appearance, is regarded as Widmanstätten ferrite. It is also interesting to note that bainitic ferrite is somehow fully grown, as far as a subunit is concerned, compared to its Widmanstätten ferrite counterpart, which is still in its early stage.

The transition from bainite to Widmanstätten ferrite can be better observed in the absence of pearlite formation. The Lower-carbon-containing alloy L2 is, therefore, an ideal

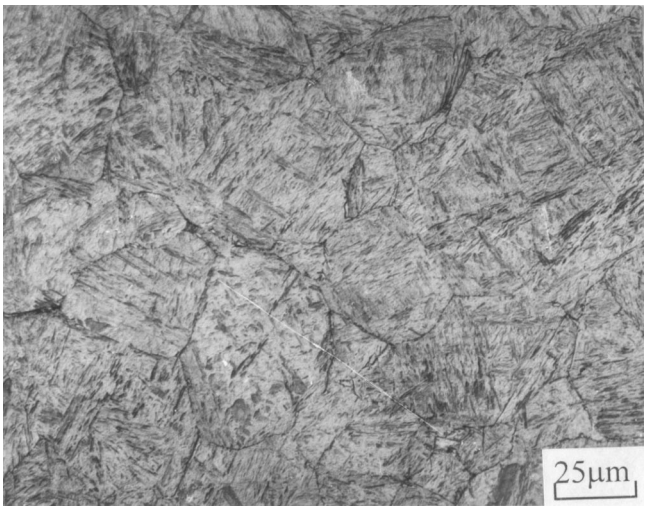

(*a*)

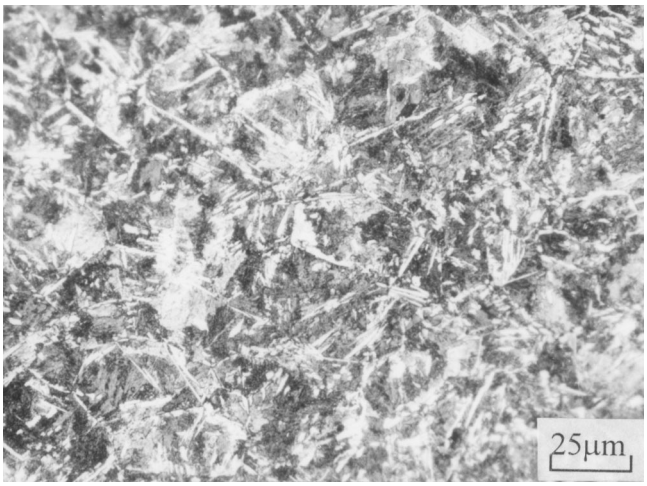

(*b*)

Fig. 3—Optical micrographs showing the microstructures of alloy H1 reacted at 510 °C for (*a*) 120 s and (*b*) 7200 s.

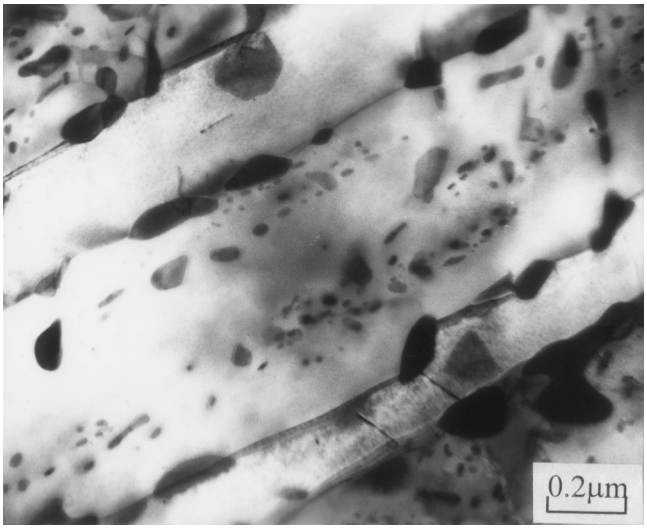

Fig. 4—TEM bright-field image showing the microstructure of alloy H1 after transforming at 510 °C for 7200 s. Carbide precipitates can be observed between the ferritic subunits.

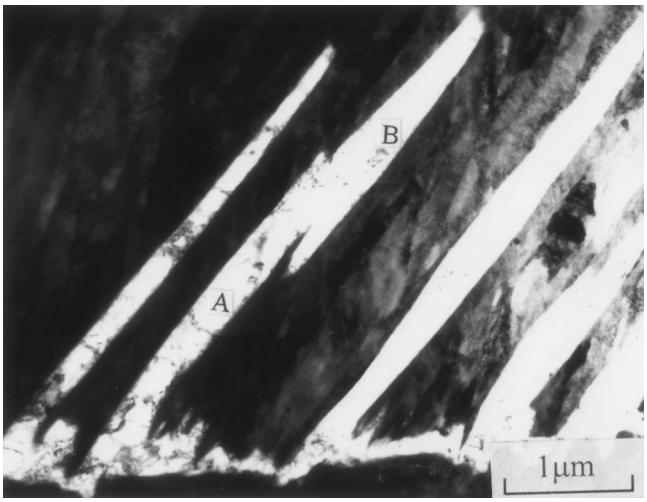

(*a*)

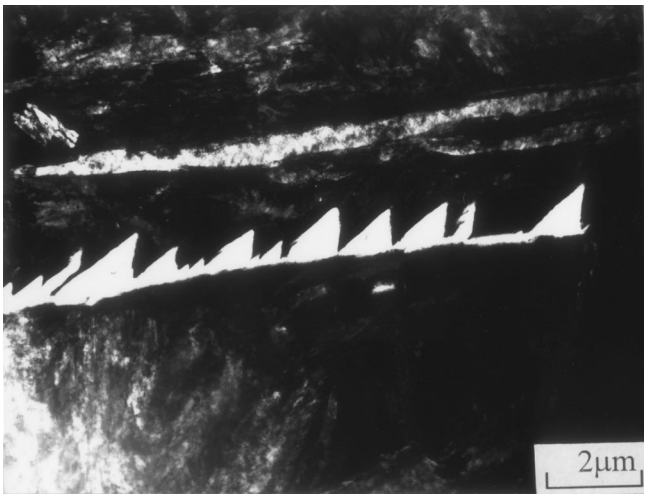

(*b*)

Fig. 5—TEM bright-field images showing (*a*) lenticular bainite and (*b*) wedgelike Widmanstätten ferrite of alloy H1 reacted at 510 °C for 120 s. The sympathetic nucleation of one subunit of bainite, B, from the tip of subunit A can be unequivocally observed in (a).

candidate. The optical micrographs of microstructures reacted at 460 °C, 480 °C, 500 °C, 520 °C, and 540 °C are shown in Figure 6. It is clear, from Figure 6, that a fully bainitic microstructure is obtained at 460 °C, while the sole product at 540 °C is Widmanstätten ferrite. The TEM investigations showed that Widmanstätten ferrite and bainite can both be found at 480 °C, even at the very early stage (10 seconds) of transformation (Figures 7(a) and (b)). Bainitic ferrite does not change its appearance in later reactions as far as the subunit is concerned (Figure 8(a)); on the other hand, Widmanstätten ferrite seems to grow bigger, although it is not fully developed, after 800 seconds (Figure 8(b)). These findings are consistent with those of alloy H1, described earlier.

It has been suggested that the nucleation process is identical for Widmanstätten ferrite and bainite, which is diffusional and involves partitioning of carbon.[13] The growth condition determines which of these phases evolves from the nucleus. If the chemical free energy change exceeds the stored energy of Widmanstätten ferrite (50 J mol^{-1}) but is

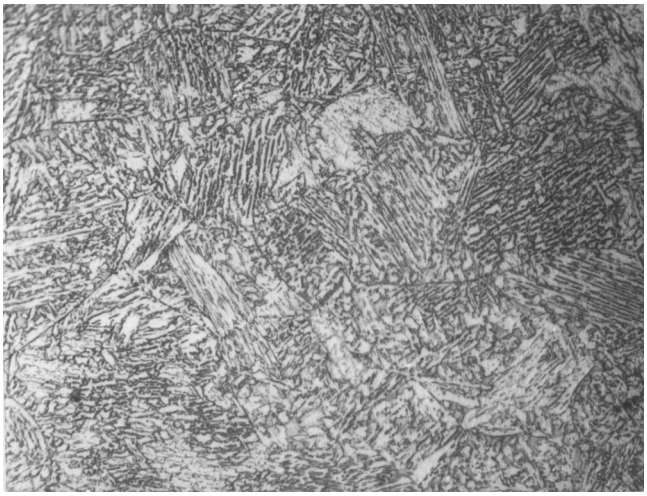

(*a*)

(*b*)

(*c*)

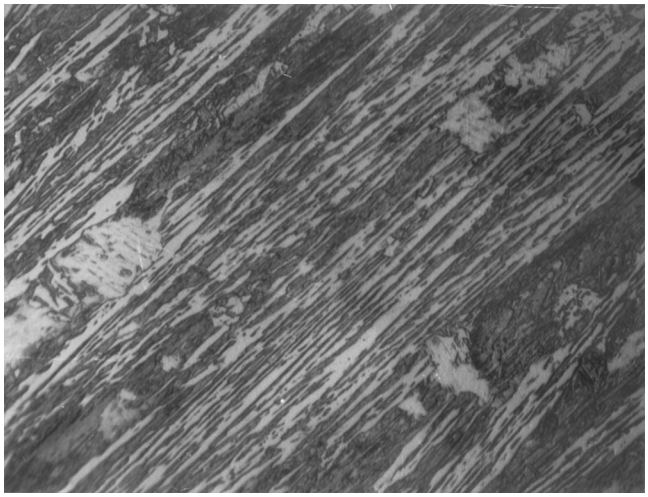

(*d*)

(*e*)

Fig. 6—Optical micrographs showing the microstructures of alloy L2 reacted across the bainite start (B_s) temperature. The samples were austenized at 1000 °C for 600 s, except the sample reacted at 520 °C, which was held at 1300 °C for 180 s. The reaction time is 800 s for all the cases: (*a*) 460 °C, (*b*) 480 °C, (*c*) 500 °C, (*d*) 520 °C, and (*e*) 540 °C.

less than that of bainite (400 J mol^{-1}), Widmanstätten ferrite will form. On the other hand, if the free energy change is larger than 400 J mol^{-1}, Widmanstätten ferrite will be replaced by bainite.[13] The observation made here indicates that, at least in a narrow temperature range, both phases can form at the same temperature even from the very beginning of the transformation.

Widmanstätten ferrite was considered to grow under paraequilibrium conditions, for which the substitutional atoms are effectively frozen but interstitial species, such as car-

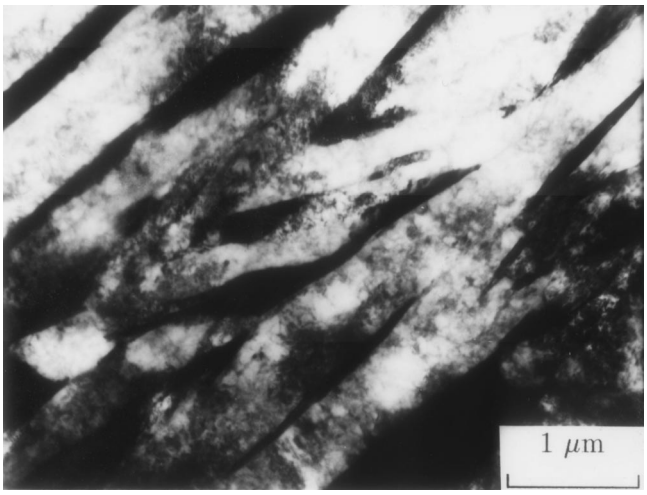

(*a*)

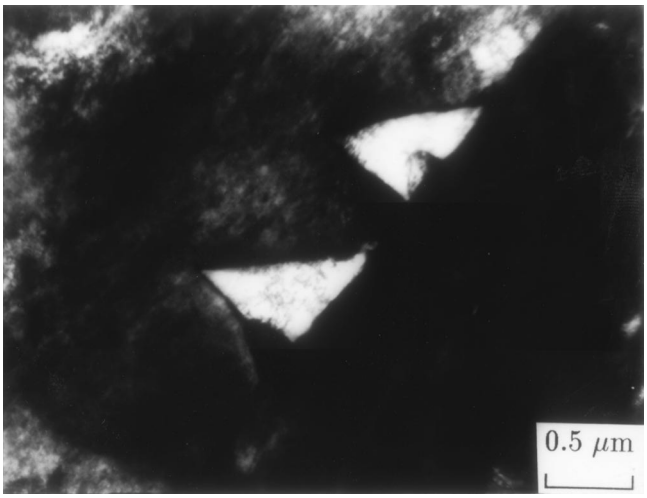

(*b*)

Fig. 7—TEM bright-field images showing the microstructures of alloy L2 reacted at 480 °C for 10 s: (*a*) bainite and (*b*) Widmanstätten ferrite.

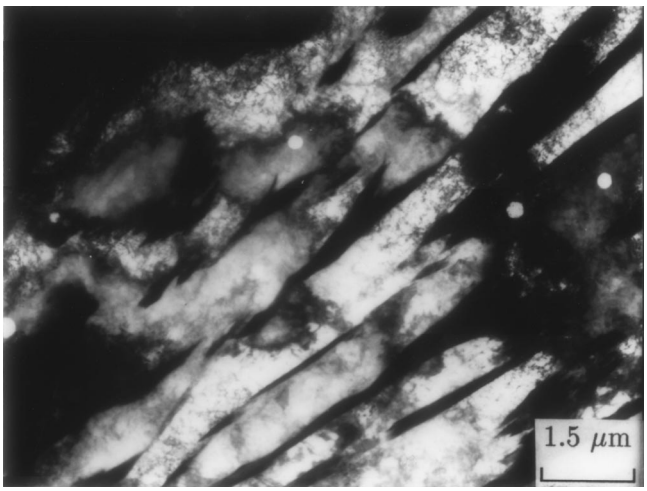

(*a*)

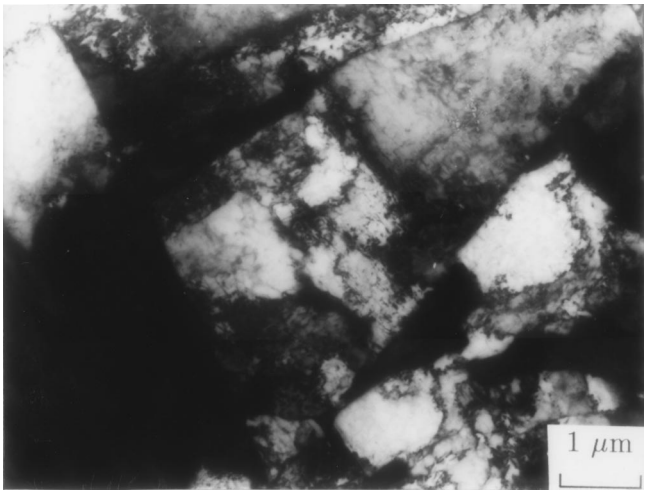

(*b*)

Fig. 8—TEM bright-field images showing the microstructures of alloy L2 reacted at 480 °C for 800 s: (*a*) bainite and (*b*) Widmanstätten ferrite. Compared with Fig. 7, morphology of bainite remains more or less identical, while Widmanstätten ferrite grows bigger as the transformation proceeds.

bon, partition according to the tie-line of the paraequilibrium phase diagram. The growth rate of Widmanstätten ferrite is, thus, controlled by the diffusion of carbon in austenite ahead of the moving interface. The growth of bainite is achieved by alternative nucleation of successive subunits. The growth rate of bainite is, therefore, largely determined by its ability to nucleate successive subunits. At a certain temperature, it is expected that bainite can grow faster than Widmanstätten ferrite. For the subunit itself, the growth rate is even faster since no diffusion is needed during the process, as is the case in martensitic transformation. The results can be interpreted such that the nuclei evolve into either phase, but bainite grows much faster than Widmanstätten ferrite.[20,21] The discrepancy of growth rates for bainite and Widmanstätten ferrite may be responsible for the observations of these phases at different stages of their growth; the bainite subunit grows to its maximum size while Widmanstätten ferrite is still in its early stage. At the latter stage, the bainite sheaf can be observed, but the Widmanstätten ferrite is not yet fully grown.

C. *Theoretical Consideration of Bainite Start Temperatures*

The bainite start temperature bears a significant hint of the transformation mechanism of bainite formation. If the process of bainite reaction is indeed diffusionless, the highest temperature at which bainite can grow should be below the T_0 line, *i.e.*, $B_s < T_0$. The T_0 concept was first introduced by Zener[22] and modified by Aaronson *et al.*[23,24] A further calculation was carried out by Bhadeshia and Edmonds[21] allowing for the effect of elastic strain due to the transformation, giving a strain energy of about 400 J mol^{-1} (T_0').

A way of predicting B_s temperature is to introduce the universal nucleation function (G_N) which is determined experimentally,[25] in addition to the growth criterion (T_0') described previously. Nucleation of bainite is possible only when the maximum free energy change accompanying the nucleation ($| G_M |$) is larger than $| G_N |$. Thus, the B_s temperature for a given alloy can be predicted to be the lower

Table III. The Measured Bainite Start Temperatures (B_s) and the Corresponding T_0, T_0', and Calculated B_s Temperatures of the Experimental Alloys (°C)

Alloy	Measured B_s	T_0	T_0'	Calculated B_s
L1	460	570	450	526
L2	470	625	510	480
M1	400	570	460	380
M2	460	620	480	380
M3	540	630	510	500
M4	450	510	420	440
H1	510	515	425	380
H2	450	710	540	380

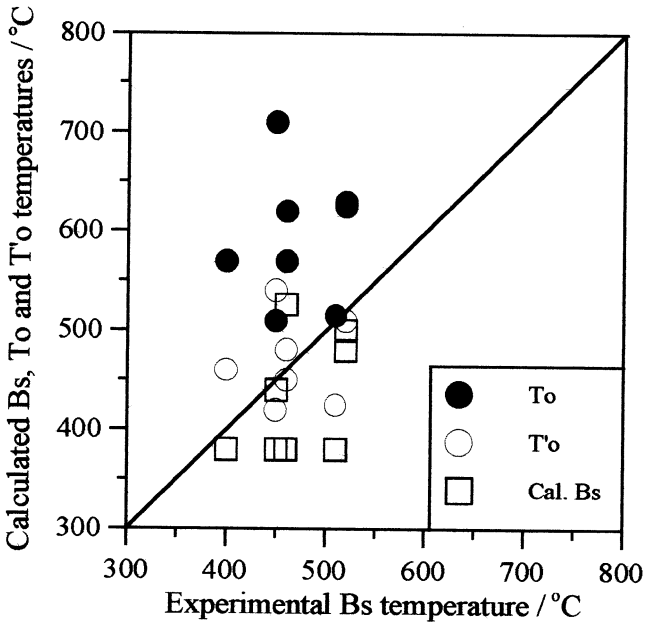

Fig. 9—The experimental B_s temperatures are plotted against predicted values; comparisons with the corresponding T_0 and T_0' data are also included.

value of its corresponding T_0' temperature or the temperature at which $| G_M |$ is larger than $| G_N |$. The determined B_s temperatures of the experimental alloys, along with the corresponding T_0', T_0', and calculated B_s temperatures, are tabulated in Table III and are also plotted in Figure 9 for the purpose of comparison. It is clear that all the experimental B_s temperatures lie below the corresponding T_0 curve. The results also indicate that reasonable agreement has been achieved between the (LB_s) curve and the predicted B_s temperatures. This is consistent with the displacive mechanism of bainite formation.

D. *Lower Bainite Start Temperatures*

It is interesting that in all cases, the lower bainite start (LB_s) temperature is found to be quite close to the corresponding martensite start (M_s) temperature (Table II). The silicon, which is contained in all the steels examined, has the effect of retarding cementite precipitation[15] and appears to be responsible for depressing the LB_s temperature. It has been suggested[10] that there is no fundamental difference in the transformation mechanism for these two forms of bainite. The bainitic ferrite grows supersaturated with carbon. The excess carbon may then partition into the residual austenite or precipitate in the ferrite in the form of carbides. If the latter process is dominant, lower bainite is obtained. Upper bainite is obtained only when carbon partitions relatively rapidly into the residual austenite, before the carbides have an opportunity to precipitate. The presence of silicon in steel will, therefore, prolong the time for the precipitation of cementite and favor the formation of upper bainite. Several recent results also exhibit the similar trend of lowering the LB_s temperature for the silicon-containing steels.[3,26,27] Furthermore, it is possible for silicon to retard the formation of lower bainite in the entire bainite-formation temperature.[26] These results are consistent with the model described previously.

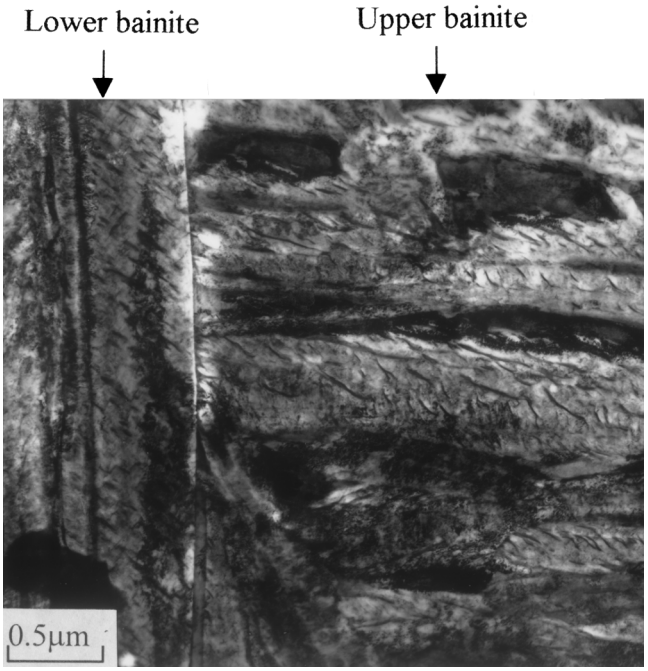

Fig. 10—TEM bright-field image showing the mixed microstructure of upper and lower bainite of alloy H1 reacted at 290 °C for 3000 s.

According to this model, it is also possible to form a mixed microstructure of upper and lower bainite in a narrow temperature range around the LB_s temperature. This is because the carbon enrichment of the austenite caused by upper-bainitic transformation can result in the subsequent formation of lower bainite.[10] The mixed microstructure of both forms of bainite is, indeed, observed here; a typical micrograph is shown in Figure 10. It is noted that a lower bainite plate contains one major and some minor variants of carbide precipitates in the right-hand side of the micrograph. However, in the left-hand side, several upper bainite sheaves can be found. There are numerous curved retained austenite films inside each upper bainite sheaf.

Regression analysis was conducted to compare the effects of alloying elements, silicon in particular, on the LB_s temperature. The present data and those from Llopis,[28] and Pickering[29] gave the following equation, which is illustrated in Figure 11:

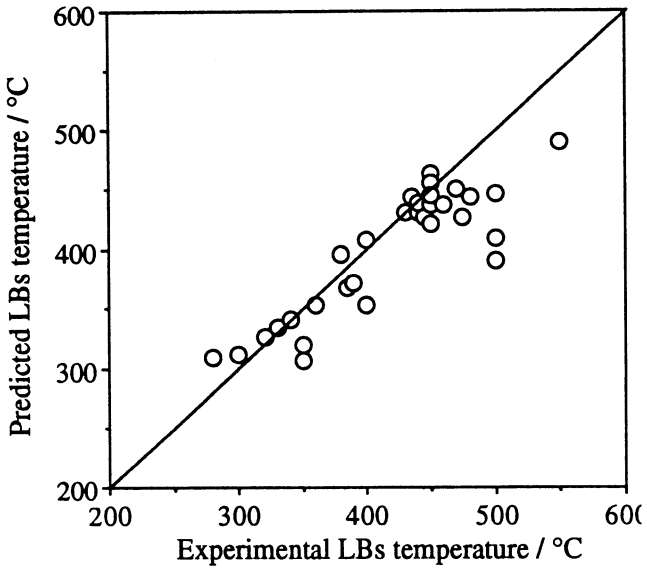

Fig. 11—A comparison of the experimental lower bainite start temperatures against calculated values obtained from linear regression analysis (Eq. [1]).

$$LB_s\ (°C) = 500 - (155 \pm 40)\ C - (38 \pm 14)\ Si - (17 \pm 13)\ Mn - (4 \pm 11)\ Ni - (10 \pm 13)\ Cr - (5 \pm 20)\ Al - (4 \pm 56)\ Co$$

where the compositions of all the elements are in weight percent. The correlation coefficient (R) of 0.89 indicates rather good correlation. Silicon clearly depresses the LB_s temperatures more effectively than any other element except carbon.

IV. CONCLUSIONS

The bainite start temperatures of eight Si-containing steels were found to be lower than the corresponding T_0 temperature, consistent with the considered displacive mechanism of bainite formation. The coformation of Widmanstätten ferrite and bainite occurs near the B_s temperature, although the growth of Widmanstätten ferrite clearly lagged behind that of bainite. This is not inconsistent with the suggestion that, while Widmanstätten ferrite and bainite develop from identical nuclei, their growth processes are different: the growth rate of the displacive formation of bainite is faster than that of Widmanstätten ferrite *via* a paraequilibrium condition.

Lower-bainite start temperatures were observed to be very close to the corresponding M_s temperatures; thus, the effect of silicon in depressing the formation of bainite is confirmed. Upper and lower bainite can also be found in the sample reacted near the LB_s temperature. It therefore supports the idea that the transition of upper/lower bainite is merely a kinetic competition between carbon partitioning into austenite and carbide precipitation inside ferrite.

REFERENCES

1. R.F. Hehemann, K.R. Kinsman, and H.I. Aaronson: *Metall. Trans.*, 1972, vol. 3, pp. 1077-93.
2. H.I. Aaronson: *The Mechanism of Phase Transformations in Crystalline Solids*, Institute of Metals Monograph 33, Institute of Metals, London, 1986, pp. 270-81.
3. H.K.D.H. Bhadeshia and D.V. Edmonds: *Metall. Trans. A*, 1979, vol. 10A, pp. 895-907.
4. W.T. Reynolds, Jr., H.I. Aaronson, and G. Spanos: *Mater. Trans. JIM*, 1991, vol. 32, pp. 737-46.
5. G.J. Shiflet and H.I. Aaronson: *Metall. Mater. Trans. A*, 1990, vol. 21A, pp. 1413-32.
6. W.T. Reynolds, Jr., F.Z. Li, C.K. Shui, and H.I. Aaronson: *Metall. Trans. A*, 1990, vol. 21A, pp. 1433-63.
7. H.I. Aaronson, W.T. Reynolds, Jr., G.J. Shiflet, and G. Spanos: *Metall. Trans. A*, 1990, vol. 21A, pp. 1343-80.
8. Y. Ohmori and T. Maki: *Mater. Trans. JIM*, 1991, vol. 32, pp. 631-41.
9. H.K.D.H. Bhadeshia: *Bainite in Steels*, The Institute of Materials, London, 1992, pp. 117-21.
10. M. Takahashi and H.K.D.H. Bhadeshia: *Mater. Sci. Technol.*, 1990, vol. 6, pp. 592-603.
11. N.F. Kennon and N.A. Kaye: *Metall. Trans. A*, 1982, vol. 13A, pp. 975-78.
12. J.M. Oblak and R.F. Hehemann: *Transformation and Hardenability in Steels*, Climax Molybdenum Co., Ann Arbor, MI, 1967, pp. 15-30.
13. H.K.D.H. Bhadeshia: *Acta Metall.*, 1981, vol. 29, pp. 1117-30.
14. Y.C.J. Jung, K. Nakai, H. Ohtsubo, and Y. Ohmori: *Iron Steel Inst. Jpn.*, 1994, vol. 34 (1), pp. 43-50.
15. W.S. Owen: *ASM Trans.*, 1954, vol. 11, pp. 812-28.
16. H.K.D.H. Bhadeshia: *J. Phys.*, 1982, vol. 43, pp. C4-437-C4-441.
17. R.F. Hehemann: *Phase Transformation*, ASM, Metals Park, OH, 1970, pp. 397-432.
18. H.I. Aaronson and C. Wells: *Trans. AIME*, 1956, vol. 256, pp. 1216-23.
19. H.K.D.H. Bhadeshia and J.W. Christian: *Metall. Trans. A*, 1992, vol. 21A, pp. 767-97.
20. H.K.D.H. Bhadeshia: *Mater. Sci. Technol.*, 1985, vol. 1, pp. 497-504.
21. H.K.D.H. Bhadeshia and D.V. Edmonds: *Acta Metall.*, 1980, vol. 28, pp. 1265-73.
22. C. Zener: *Trans. TMS-AIME*, 1946, vol. 167, pp. 550-59.
23. H.I. Aaronson, H.A. Domian, and G.M. Pound: *Trans. TMS-AIME*, 1966, vol. 236, pp. 753-67.
24. H.I. Aaronson, H.A. Domian, and G.M. Pound: *Trans. TMS-AIME*, 1966, vol. 236, pp. 768-80.
25. A. Ali and H.K.D.H. Bhadeshia: *Mater. Sci. Technol.*, 1989, vol. 5, pp. 398-402.
26. K. Tsuzaki, C. Fujiwara, and T. Maki: *Mater. Trans. JIM*, 1991, vol. 32, pp. 658-66.
27. V.T.T. Miihkinen and D.V. Edmonds: *Mater. Sci. Technol.*, 1987, vol. 3, pp. 422-31.
28. A.M. Llopis: Ph.D. Thesis, University of California, Berkeley, CA, 1977.
29. F.B. Pickering: *Transformation and Hardenability in Steels*, Climax Molybdenum Co., Ann Arbor, MI, 1967, pp. 109-32.